

Atomic Detail Peptide-Membrane Interactions: Molecular Dynamics Simulation of Gramicidin S in a DMPC Bilayer

Dan Mihailescu^{*†} and Jeremy C. Smith[†]

^{*}Faculty of Biology, University of Bucharest, 76201 Bucharest, Romania; and [†]Lehrstuhl für Biocomputing, IWR, Universität Heidelberg, D-69120 Heidelberg, Germany

ABSTRACT Molecular dynamics simulations have been performed of the sequence-symmetric cyclic decapeptide antibiotic gramicidin S (GS), in interaction with a hydrated dimyristoylphosphatidylcholine (DMPC) bilayer, and the results compared with a “control” simulation of the system in the absence of GS. Following experimental evidence, the GS was initially set in a single antiparallel β -sheet conformation with two Type II' β -turns in an amphiphilic interaction with the membrane. This conformation and position remained in the 6.5 ns simulation. Main-chain dihedrals are on average $\sim 26^\circ$ from those determined by NMR experiment on GS in dimethylsulfoxide (DMSO) solution. Sequence-symmetric main-chain and side-chain dihedral angle pairs converge to within $\sim 5^\circ$ and $\sim 10^\circ$, respectively. The area per lipid, lipid tail order parameters, and quadrupole spin-lattice relaxation times of the control simulation are mostly in good agreement with corresponding experiments. The GS has little effect on the membrane dipole potential or water permeability. However, it is found to have a disordering effect (in agreement with experiment) and a fluidifying effect on lipids directly interacting with it, and an ordering effect on those not directly interacting.

INTRODUCTION

There is much interest in understanding the interaction of peptides with lipid bilayers at atomic detail. This requires characterization of the position, orientation, structure, and dynamics of the peptide in the lipid bilayer and its effects on surrounding lipids. Although molecular dynamics (MD) simulation can in principle furnish complete structural and dynamical information, considerable obstacles exist to obtaining accurate results, due partly to inexact force fields and other approximations in simulation methodology, and partly to the relaxation times of some important dynamical phenomena being of the order of or longer than those presently accessible to MD.

Gramicidin S, [*cyclo*-(Leu-D-Phe-Pro-Val-Orn)₂], (GS)] is a cyclic decapeptide that is of particular interest for pursuing peptide/membrane MD studies. The sequence and structure of the peptide are relatively simple. NMR, x-ray, and MD studies indicate that the backbone adopts an antiparallel β -sheet with two Type II' β -turns in various solutions of different polarity and in the crystalline form (Jones et al., 1978; Hull et al., 1978; Mihailescu and Smith, 1999). One consequence of this is that the GS structure is amphipathic, with the hydrophobic side chains on one side of the molecule and the hydrophilic ones on the other, and this provides a logical geometry for interaction with a lipid membrane, with the polar side of GS at the lipid/water interface and the nonpolar side interacting with the lipid tails. Considerable experimental evidence exists that this is

indeed the case and a variety of biophysical studies on the interaction of GS with model lipid membranes have confirmed that it interacts primarily with the headgroup and interfacial polar/apolar regions (Datema et al., 1986; Zidovetzki et al., 1988; Prenner et al., 1997; Higashijima et al., 1986). The sequence symmetry also provides a natural test of convergence of certain properties in the simulation which, when time-averaged, should be identical for the two halves of the molecule.

Also of interest is that GS has antibiotic action via membrane ion permeability change (Katsu et al., 1989; Portlock et al., 1990). For this reason over 200 analogs have been synthesized with the aims of better-defining its structure-activity properties and extending the activity of the compound to produce a more potent and specific antibiotic. The presence of the amphipathy (or “sidedness”) and the β -turns appears to be required for activity (Katsu et al., 1987).

Although a complete description of how GS induces ion permeability is probably beyond the capability of present-day simulation methods, they can be used to provide information on how GS interacts with and perturbs lipid bilayers under simple controlled conditions. In initial simulation work we performed a 5-ns MD calculation of GS in DMSO solution, enabling detailed comparison with NMR results in the same solvent (Mihailescu and Smith, 1999). Here we extend this work to an analysis of the interaction of GS with a hydrated DMPC membrane bilayer. DMPC was chosen as a well-studied model system, and because NMR data exist on the disordering effect of GS on DMPC lipid bilayers.

We report on two MD simulations, one of GS in interaction with a hydrated DMPC bilayer and a “control” simulation of a hydrated DMPC bilayer in the absence of GS. The control simulation is used to check the validity of the simulation method with respect to spectroscopic and dif-

Received for publication 10 December 1999 and in final form 13 July 2000.

Address reprint requests to Dr. Jeremy C. Smith, Lehrstuhl für Biocomputing, IWR, Universität Heidelberg, Im Neuenheimer Feld 368, D-69120 Heidelberg, Germany. Tel.: 49-6221-54-88-57; Fax: 49-6221-54-88-68; E-mail: biocomputing@iwr.uni-heidelberg.de.

© 2000 by the Biophysical Society

0006-3495/00/10/1718/13 \$2.00

fraction data, and to use for comparison of the lipid molecule structure and dynamics in the presence and absence of GS.

METHODS

Two simulations were performed, one of GS interacting with a hydrated DMPC bilayer (subsequently called the “GS/DMPC” simulation) and one of a hydrated pure DMPC bilayer (subsequently called the “control” simulation).

The effect of GS on membranes varies with lipid composition, and ^{13}P -NMR and x-ray diffraction have provided evidence for lipid polymorphism in gramicidin S-lipid systems (Prenner et al., 1997). However, both in the gel and liquid-crystalline states hydrated DMPC doped with GS exists exclusively as a bilayer (Prenner et al., 1997). In the present GS/DMPC simulation the microscopic system is a single GS molecule interacting with a hydrated DMPC bilayer with 38 molecules of DMPC (17 in the layer containing GS (the “GS” layer) and 21 in the layer not containing GS (the “non-GS” layer) and 1666 water molecules, i.e., a total of 9656 atoms. The resulting lipid/GS ratio (38:1) is far higher than that at which GS destroys bilayers: total bilayer disruption occurs only at ratios of <3:1 (Zidovetzki et al., 1988). At 25:1 the DMPC membranes are still in bilayer form (Prenner et al., 1997).

A “control” simulation, of DMPC without the peptide, was also performed. The control system consisted of 42 DMPC molecules and 1734 water molecules i.e., a total of 10,158 atoms. For consistency, both simulations started with the same primary box dimensions: $37 \times 37 \times 70.6 \text{ \AA}^3$. Consequently, the number of water molecules is slightly different in the two systems.

System size effects must be considered. Although these may influence bilayer and peptide insertion properties, there is some indication that the system size chosen is reasonable for the present purposes. First, MD simulation studies on hydrated DMPC bilayers with different numbers of lipid molecules per monolayer have indicated that a bilayer of 18 DMPC molecules per monolayer is sufficient for characterizing many bilayer properties (Stouch, 1993). Moreover, the water/lipid ratio in the present work is 44:1, well above the ratio of 20.5:1, above which the bilayer structure does not noticeably change with hydration (Marrink et al., 1993). X-ray experiments suggest that the basic structural characteristics of the dipalmitoyl phosphatidylcholine (DPPC) bilayer are maintained even at 15.3 waters/lipid (Nagle et al., 1996).

In what follows the membrane normal is oriented along the z axis and the center of the bilayer is at $z = 0$. The x and y axes are therefore parallel to the membrane plane. Periodic rectangular boundary conditions were applied in the x and y directions to simulate an infinite planar layer and in the z direction to simulate a multilayer system.

The program used was CHARMM Version 26 (Brooks et al., 1983). The all-atom CHARMM force field version 22.0 was used for the lipids (Schlenkerich et al., 1996) and all peptide (MacKerell et al., 1998) residues except Orn. The force field for Orn, which is the same as Lys except that it has one less CH_2 group, was published in Mihailescu and Smith (1999). The water model was TIP3P (Jorgensen et al., 1983) modified as in current use in CHARMM. The electrostatic interactions were smoothed using the SWITCH method (Brooks et al., 1983), which involves multiplication by a cubic function, in this case between 8 and 12 \AA . During the NVE and NPT dynamics bond lengths involving hydrogen atoms were constrained with the SHAKE algorithm, thus allowing the use of a time step of 2 fs.

There are various ways of treating macroscopic boundary conditions in MD, discussed in the case of lipid bilayer systems by Tieleman et al., 1997. Two of the most frequently used are N (number of molecules) V (volume) E (energy), and N (number of molecules) P (pressure) T (temperature) in which the named parameters are kept constant during the simulation. Constant pressure algorithms allow the surface area per lipid to vary, and thus be compared with experiment. Another property to be considered is the surface tension. It has been pointed out that if the surface tension of the

bilayer membrane is not zero the membrane, if free to compress or expand, will adopt a state in which the attractive and repulsive interactions balance each other (Jähnig, 1996). In this situation the free energy is minimal with respect to the area of the membrane, and the derivative of the free energy with respect to the area, the surface tension, will vanish. However, long wavelength undulations, intrinsically associated with the value of the macroscopic surface tension, are absent in a simulation cell that is constrained by periodic boundary conditions. To reduce the consequences of this system size effect, a small surface tension might therefore be appropriate, even if the macroscopic tension should be zero (Feller and Pastor, 1996). However, direct comparison of membrane simulations with (28 mN/m) and without surface tension revealed no significant differences in the results (Tieleman and Berendsen, 1996). In the present work no surface tension was applied.

We choose here NPT conditions, allowing the box dimensions to vary. The Langevin piston algorithm was used (Feller et al., 1995). This method is appropriate for inhomogeneous systems such as aqueous biopolymers, liquid/liquid interfaces, and lipid bilayers containing peptides, for two reasons. First, for such systems no large temperature difference between the components of the system is created, and therefore it is not necessary to couple the different components to separate heat baths. Second, the method has the advantage of not being critically dependent on the choice of the piston parameters.

The method for constructing the initial configuration of the GS/DMPC system and the equilibration mostly follows that used in the simulation of Gramicidin A/DMPC (Woolf and Roux, 1994, 1996) and described in Roux and Woolf (1996). The main steps were as follows.

GS/DMPC simulation

Initial system geometry

An initial equilibration was performed at 330 K, higher than the final simulation temperature (305 K) to allow increased exploration of the local conformational space. To derive an initial geometry for this simulation the area per lipid was taken as 64 \AA^2 , estimated by extrapolation from the experimental values of $59.6 \pm 0.5 \text{ \AA}^2$ at for DMPC at 30° (Petrache et al., 1998; König et al., 1997) and $62.9 \pm 1.3 \text{ \AA}^2$ for DPPC at 50°C (Nagle et al., 1996). The cross-sectional area of the GS was calculated using the method of Lee and Richards (1971) to be $\sim 258 \text{ \AA}^2$ and, using the value of 64 \AA^2 for the DMPC cross-section, the layer containing GS should then contain four lipids fewer than the layer without GS.

The starting conformation of GS was chosen as one of the most C_2 -symmetric geometries obtained in the preliminary MD study of GS in DMSO (Mihailescu and Smith, 1999). This conformation was positioned with the Orn δ N atoms at $z = 17 \text{ \AA}$, with the plane defined by the heavy atom backbone of GS placed parallel to the membrane plane and the associated symmetry axis parallel to the z axis. This insertion geometry is consistent with a variety of biophysical experiments on GS/membrane interactions and satisfies the amphiphilicity of the molecule, with the Orn residue side chains at the polar interface and the hydrophobic side chains interacting with the lipid hydrophobic tails (Davis et al., 1983; Katsu et al., 1987). Moreover, in this way both phenylalanines are also at the lipid/water interface. The presence of aromatic amino acids such as tryptophan, tyrosine, and phenylalanine near the interfacial region is a feature of several membrane proteins (see Woolf and Roux, 1996 and references therein; and Woolf, 1998).

To determine the position of each of the 17 lipids in the GS-containing layer and 21 lipids in the non-GS layer, the polar headgroups were represented as spheres of cross-sectional area 64 \AA^2 . The positions of the spheres were constrained at $z = 17 \text{ \AA}$ (the same level as the Orn δ N atoms) for the upper layer and $z = -17 \text{ \AA}$ for the lower layer. Short energy minimization and Langevin dynamics runs were used to arrange the spheres around the peptide and to obtain the desired dimensions of the system. The van der Waals parameters of the spheres approximated the polar group of the lipid molecule.

The spheres were substituted by all-atom DMPC molecules, randomly chosen from a library of 2000 preequilibrated and prehydrated (with ~20 water molecules) lipids, obtained by empirically adjusting the force field parameters to reproduce experimental deuterium quadrupolar splitting order parameters and ^{13}C -NMR relaxation times of the acyl chains (Venable et al., 1993). The center of any given sphere was used to place the center of mass of the phosphorus and nitrogen atoms of the corresponding lipid polar head.

Rigid-body rotations of the lipids around the z axis and translations in the xy plane were performed to minimize the number of unfavorable contacts and atomic overlaps. The remaining bad contacts were removed by energy minimization.

The system was then fully hydrated by overlaying a preequilibrated water box of the appropriate dimensions in the x and y directions. The resulting starting conformations for the DMPC/GS and control primary simulation boxes are shown in Fig. 1.

Initial all-atom equilibration

A number of position constraints were used at the beginning of the ensuing equilibration period to ensure a smooth relaxation of the system toward an equilibrated configuration. Harmonic constraints were initially applied to all the atoms of GS to prevent its changing position and orientation in the bilayer, and the polar headgroups of the lipids were kept around $z = \pm 17$ Å using planar harmonic constraints of the form $V = k(d - d_0)^2$, where k is the force constant (5.0 kcal/mol/Å^2), d is the distance from the plane to each atom at a given time, and d_0 is the same distance in the initial frame. A similar planar potential was applied to the water atoms to prevent their penetration into the bilayer region.

The above constraints were gradually reduced during 125 ps of Langevin dynamics equilibration, performed with a friction coefficient of 3.0 ps^{-1} applied to all non-hydrogen atoms. A further 25 ps of equilibration was performed without the Langevin bath.

NVE equilibration

Following the constrained equilibration, a 3 ns NVE equilibration at $330 \pm 4 \text{ K}$ was performed. During this equilibration step a cylindrical potential was applied to all the atoms of DMPC and GS to prevent drift of the lipids and peptide. This was of the form $k(r - r_0)^2$ with $k = 5.0 \text{ kcal/mol/Å}^2$, and where r is the distance of any given atom from an axis parallel to z .

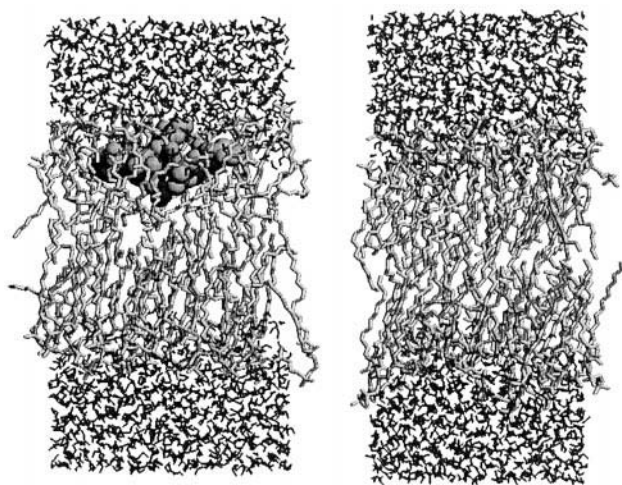


FIGURE 1 Starting configurations for DMPC/GS (left) and control membrane simulations (right). The hydrogen atoms are not shown.

NPT equilibration

After the NVE equilibration an NPT equilibration was performed and the dimensions of the orthorhombic cell were monitored. The constraints on the lipids were removed but those on the peptide were kept to prevent it drifting. For this simulation step the parameters were the following: the mass of the pressure piston was 100.0 amu, the Langevin piston collision frequency was 10.0 ps^{-1} , and the thermal piston mass was 250.0 kcal ps^2 . An isotropic pressure of 1 atm was applied. The temperature was kept constant at 305 K, above the gel-to-fluid phase transition midpoint temperature of the system ($297 \pm 0.2 \text{ K}$) and at the same temperature as in the DMPC + GS NMR study to which certain results are compared (Zidovetzki et al., 1988). After 0.5 ns of NPT equilibration the simulation box dimensions appeared to have equilibrated (see Results).

NPT production

Three ns of NPT production dynamics were run, with no constraints. This production was used for the analysis.

Control simulation

For the control simulation the same steps as above were performed apart from the NVE dynamics, which was not needed because the lipids were chosen from an already preequilibrated library (Venable et al., 1993). After equilibration at 330 K an NPT dynamics run at 305 K was performed. Again, the dimensions of the dynamic cell were monitored. After 0.75 ns these dimensions had reached approximate plateaus (Fig. 2, right panels). The equilibration was continued until 0.9 ns. The NPT was continued for another 2.0 ns production, which was used for the subsequent analysis.

The coordinates were saved every 50 steps. A total of 9.55 ns were run, taking approximately 4320 Central Processing Unit hours on a cluster composed of four dual Pentium II/450 MHz nodes, running in parallel, using the LINUX operating system. The analysis of the non-bonded interaction energies between GS and each DMPC molecule required a further 240 h of CPU.

RESULTS

GS structure and dynamics

Position and orientation of GS

The position and orientation of GS relative to the bilayer during the equilibration and production periods are shown in Fig. 2, *A* and *B*. Fig. 2 *A* presents the projections of the normal to the plane fitted to the backbone heavy atoms of GS. This plane can be described by the equation $lx + my + nz = p$. If \mathbf{n} is the vector normal directed through the plane from the origin of the Cartesian axes (x, y, z), then l, m, n are the axis projections of \mathbf{n} and p is the projection of \mathbf{r} on \mathbf{n} , where \mathbf{r} is the position vector of a point on the plane relative to the origin of the axis.

During the NVE equilibration GS diffused into the bilayer, with its center of mass 3–4 Å deeper into the hydrophobic core than at the beginning of the equilibration (Fig. 2 *B*). A tilt of the GS backbone plane relative to the z axis (the n projection) was also observed during this phase. After ~1 ns of NVE equilibration the GS molecule regained its initial membrane/water interfacial position with the backbone and membrane planes parallel to each other (n projec-

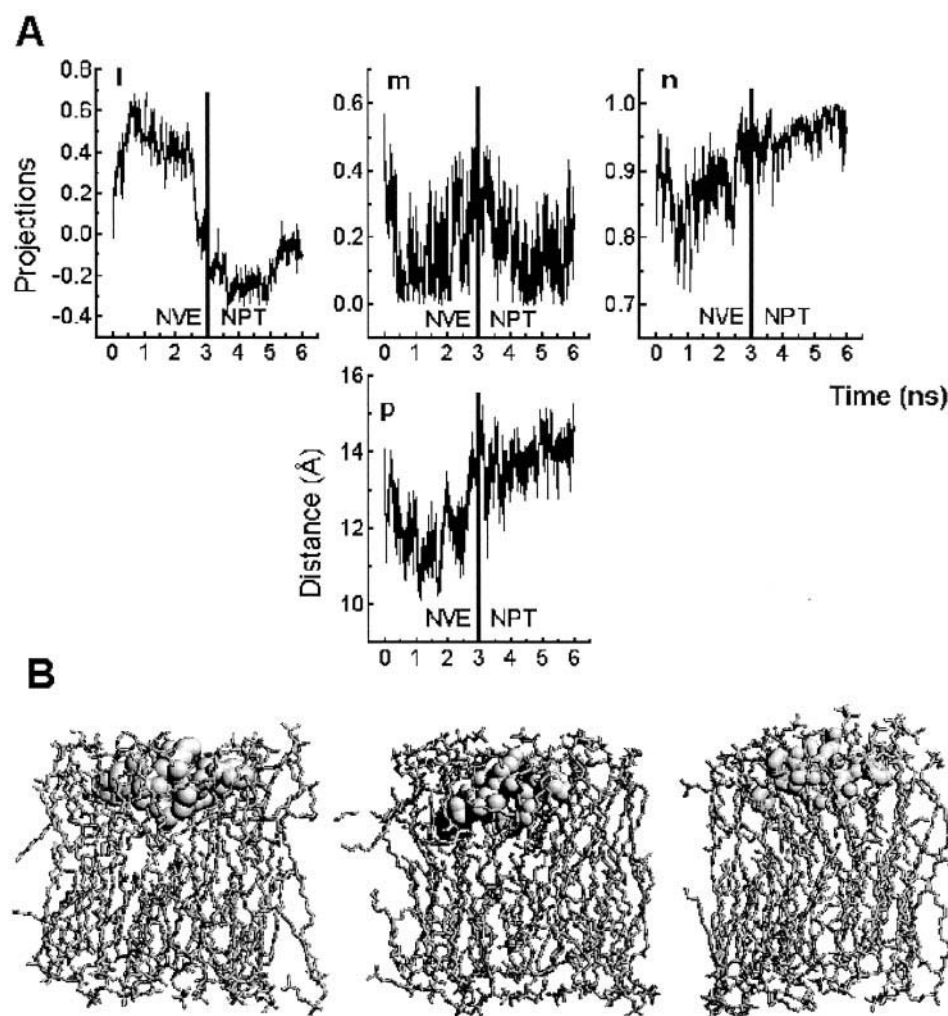


FIGURE 2 (A) Time series of the projections of GS backbone plane on the main coordinates of simulation system and of the z coordinate of the backbone atom center of mass (p). The 0.5 ns NPT equilibration between the 3 ns, NVE, and the 3 ns NPT dynamics is not shown. (B) Snapshots showing the position of GS at the beginning of the calculation, after 1.0 ns of NVE equilibration (when the GS plane was most tilted) and at the end of the NPT dynamics.

tion ≈ 1). During the 3.0 ns NPT production dynamics the average position of GS relative to the membrane remained practically unchanged.

Backbone structure and H-bonding

Experiments using x-ray diffraction (Hull et al., 1978), circular dichroism (Balasubramanian, 1967), and NMR (Stern et al., 1968) and MD of GS in DMSO solution (Mihailescu and Smith, 1999) have shown that GS adopts a robust antiparallel β -sheet with two Type II' β -turns both in the crystalline form and in various solutions. This was also the case throughout the present simulation. Both experimentally and in the present and previous simulations two pairs of backbone hydrogen bonds for GS were found, involving O-Leu-1 ... NH-Val-4, O-Leu-6 ... NH-Val-9, O-Val-4 ... NH-Leu-1, and O-Val-9 ... NH-Leu-6.

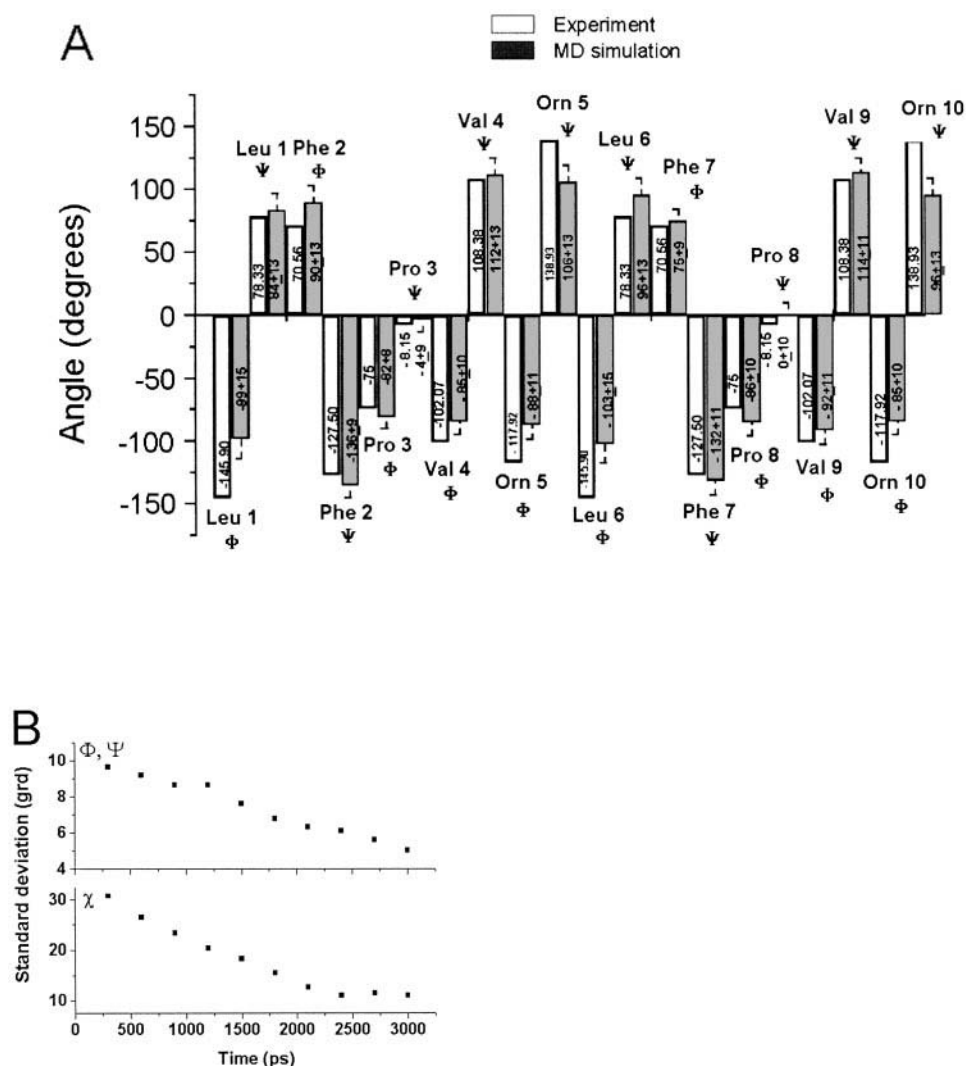
During the GS/DMPC simulation the O ... N (Leu-1 ... Val-4 and Leu-6 ... Val-9) distances were $= 3.5 \pm 0.5$ Å and 3.4 ± 0.4 Å, respectively, and those for N ... O (Leu-1 ... Val-4 and Leu-6 ... Val-9) were 2.8 ± 0.1 Å and $3.0 \pm$

0.2 Å. The values for the two members of each pair of distances are remarkably close, suggesting that this aspect of the structural symmetry of the system has converged.

Main-chain dihedrals

The main-chain dihedral angle averages are given in Fig. 3 *A* together with the corresponding NMR values of GS in DMSO solution (Xu et al., 1995). The average standard deviation between the NMR and MD values is 26° , and most dihedrals are in the same minimum as in the NMR experiment. In comparison, in the simulation of GS in DMSO solution this value was 18° , slightly closer to experiment (Mihailescu and Smith, 1999), consistent with the use of the experimental solvent, DMSO. The slightly larger deviation from the experiment in the present work may therefore be an environmental effect. As in the previous solution simulation, the backbone remains in one potential minimum during the simulation, and no conformational transitions were found for any of the backbone dihedrals. This is consistent with experimental findings for GS, which

FIGURE 3 (A) Averages and fluctuations of the main-chain dihedrals (Φ and Ψ) of GS obtained in the present work and by solution NMR (Xu et al., 1995). In the NMR study the molecule was assumed to be symmetric. (B) Standard deviations between the two halves of GS for the backbone and side-chain (χ) torsion angles during the, NVE, and NPT dynamics.



indicate that the pleated sheet structure is an extremely rigid conformation found in the crystalline form (Hull et al., 1978) and retained in solvents differing widely in their polarity (Ovchinnikov and Ivanov, 1975). ^2H -NMR data are consistent with this conformation of GS in DPPC bilayers (Datema et al., 1986).

The sequence symmetry of GS provides an intriguing opportunity to examine some convergence properties of the simulation. This can be clearly seen in Fig. 3 B, where the convergence of the values of sequence-symmetric dihedral angle pairs is shown. To examine this the equilibration and production trajectories were divided into 300-ps windows and the corresponding cumulative average angles computed. The standard deviation between sequence-symmetric angle pairs on the two halves of GS, averaged over the main-chain dihedrals and over the side-chains (χ) is plotted in Fig. 3 B. Improving convergence with time is apparent. After 3 ns the sequence-symmetric main-chain dihedrals are the same to within $\sim 5^\circ$, indicating a high degree of corre-

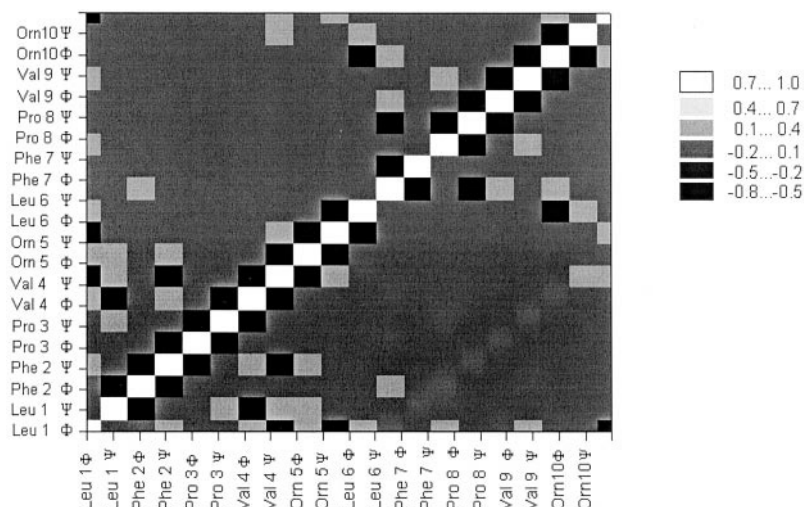
sponding structural symmetry and approximate convergence of this aspect of the simulation. The side-chain pairs of the two halves of the molecule converge to within $\sim 10^\circ$, indicating that the side-chain rotameric states are reasonably well-sampled.

In the MD simulation of GS in DMSO it was found that the fluctuations of Ψ_i and Φ_{i+1} are anticorrelated (Mihailescu and Smith, 1999). Fig. 4 indicates that similar short-range correlation effects are present for Ψ and Φ angles of GS in the DMPC bilayer.

Side-chain H-bonds

The interactions of the Orn side-chain ammonium groups are of particular interest. It has been suggested that they form salt linkages with phospholipid headgroups (Pache et al., 1972). Another possibility is the existence of hydrogen bonding between the N_δ of Orn and the CO of Phe (Hull et al., 1978; Krauss and Chan, 1982; Xu et al., 1996). If the

FIGURE 4 Grey scale domains for the correlation between the fluctuations of the Φ and Ψ dihedral angles of GS.



latter hydrogen bonding exists it may be of order $i \rightarrow I + 2$ or $i \rightarrow I - 3$, where i is the residue number. In the previous simulation work of GS in DMSO a hydrogen bond was found for one-half of the molecule, between N_δ of Orn and the CO group of the D-Phe that follows it, i.e., $i \rightarrow I + 2$ (Mihailescu and Smith, 1999). This was only partially occupied, as was found in an NMR investigation of GS in methanol (Krauss and Chan, 1982).

In the present GS/DMPC simulation the Orn side chains again interact with Phe. The donor (δN of Orn)–acceptor (O of Phe) distances are Orn-5–Phe-2, 8.3 ± 1.1 Å; Orn-5–Phe-7, 4.8 ± 1.1 Å; Orn-10–Phe-2, 5.4 ± 1.2 Å, Orn-10–Phe-7, 8.1 ± 0.8 Å. Again, the symmetry-related partners show similar distance values. Although none of the above four average values appear consistent with hydrogen-bonding, time series of the distances between δN Orn-5 . . . O Phe-7 and δN Orn-10 . . . O Phe-2 show the existence of a conformational equilibrium between hydrogen-bonded and non-hydrogen-bonded geometries (Fig. 5, *A* and *B*). The corresponding population distributions are shown in Fig. 5, *C* and *D*, together with fitted Gaussians for each of the two populated states. The Gaussians are at 4.33 ± 0.03 Å, 6.31 ± 0.02 Å, and 3.73 ± 0.03 Å, 5.59 ± 0.05 Å for the two pairs indicating the existence of very weak $i \rightarrow I + 2$ hydrogen-bonding populations. The potentials of mean force, U , determined from the probability distributions are given in Fig. 5, *E* and *F*. These exhibit two shallow wells with barriers between them of ~ 0.1 – 0.2 kcal/mol, i.e., significantly lower than $k_B T$.

Lipid structure and dynamics

Area per lipid

Time series of the dimensions of the dynamic cells for the GS/DMPC and control simulations are shown in Fig. 6. During the NPT equilibration the system sizes relax to

approximate plateaus, and in the subsequent NPT production drift only slightly. For the control system the area per lipid passes from 64 Å² at 330 K (the temperature of the NVE equilibration) to 60 Å² at 305 K (the temperature of the NPT equilibration) in 0.75 ns. For the entire 305 K control NPT production the area per lipid is 60.03 ± 0.78 Å², in good agreement with the corresponding experimental value of 59.6 ± 0.5 Å², which was obtained at a slightly lower temperature, 303 K (König et al., 1997; Petrache et al., 1998).

For the GS/DMPC system, dividing the area of the dynamic cell of the simulated system in the xy plane (membrane plane) by 21 (the number of the lipids in the non-GS layer) gives a value of 56.9 ± 0.6 Å². Therefore, the area per lipid in the non-GS layer is significantly smaller than the

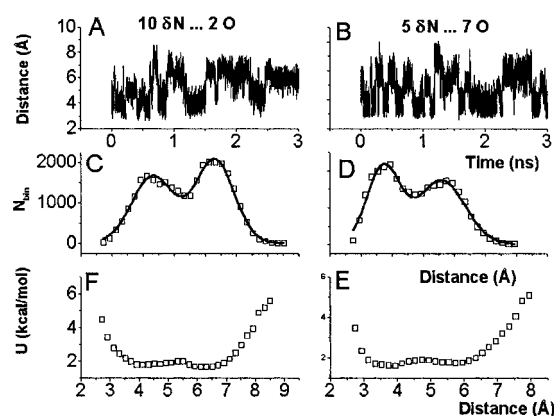


FIGURE 5 (*A* and *B*) Time series of the distances between δN atoms of Orn (5 and 10) and oxygen atoms of Phe (2 and 7). (*C* and *D*) Histogram distributions of acceptor-donor distances in 0.2 Å bin widths for 5 δN . . . 7 O and 10 δN . . . 2 O. For each distribution the best-fitted Gaussians (solid lines) for the two population peaks are also shown. (*E* and *F*) The potential of mean force derived from the probability distributions of the distances presented in *C* and *D*.

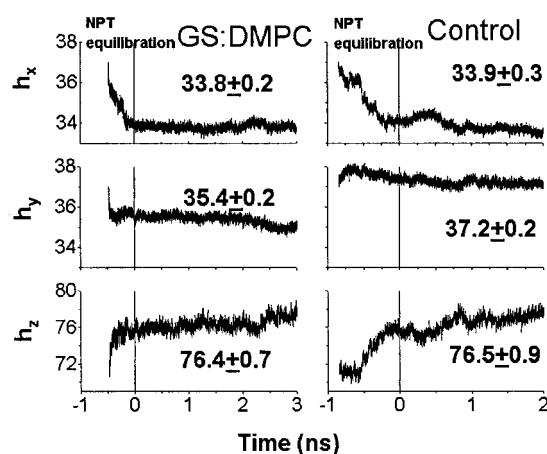


FIGURE 6 Time series of the cell dimensions (h_x , h_y , h_z) for NPT dynamics for GS/DMPC and control simulations. Vertical lines divide the NPT equilibration and production periods. The average and standard deviations of the cell dimensions during the production dynamics are also given.

values obtained for the control system in both experiment ($59.6 \pm 0.5 \text{ \AA}^2$) and simulation ($60.03 \pm 0.78 \text{ \AA}^2$).

The value obtained for the GS layer depends on the method of calculation, and in particular whether the area under the peptide is included. If it is not, i.e., only the solvent-accessible area is taken into account, then the accessible area of the GS molecule itself is calculated and subtracted. To do this, for each dynamics frame the cross-sectional area of GS was determined by computing its volume using the Lee and Richards method (Lee and Richards, 1971) in 1-Å-thick slabs normal to the z axis, and the maximal value of the area was kept. The time-averaged maximal cross-sectional area of GS was $272 \pm 11 \text{ \AA}^2$. Subtracting this from the xy area of the system and dividing the result by 17, the number of lipids in the GS layer, gives a value of $54 \pm 2 \text{ \AA}^2$, which is again smaller than in the control system. However, if the volume under the peptide, which is also occupied by lipid chains, is included then the area per lipid increases to $\sim 70 \text{ \AA}^2$ in non-GS layer. Averaging over lipids in both layers then gives 63 \AA^2 , indicating an apparent increase in the area per lipid relative to the control.

Headgroup atom distributions

Headgroup atom distributions along the bilayer normal (z axis) are shown for both monolayers in the GS/DMPC and control simulations in Fig. 7. Following Essemann and Berkowitz (1999) to quantify the degree of symmetry between the two layers of the membrane, the distribution functions obtained for each layer were fitted with Gaussian functions and the positions and widths of the Gaussians compared. For the control simulation the widths were $3.88 \pm 0.20 \text{ \AA}$ and $3.67 \pm 0.29 \text{ \AA}$ for O, $3.61 \pm 0.31 \text{ \AA}$ and

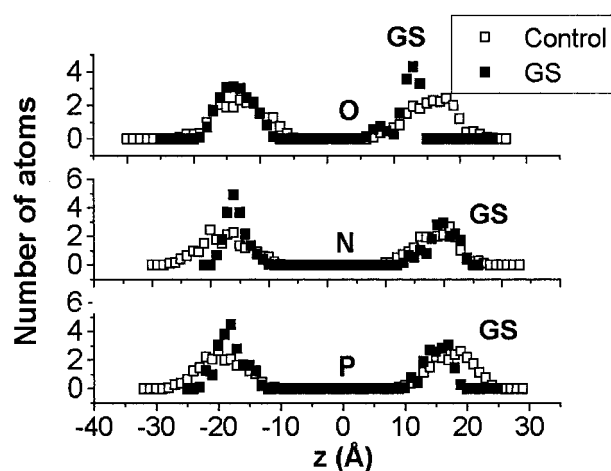


FIGURE 7 DMPC atom distributions for carboxylic oxygen, nitrogen, and phosphorus GS/DMPC (■) and control (□). To obtain these the systems were divided into 1 Å bins and the time-averaged numbers of atoms calculated. The size of the symbols corresponds to the highest fluctuation of the values.

$4.44 \pm 0.45 \text{ \AA}$ for N, and $3.83 \pm 0.25 \text{ \AA}$ and $3.72 \pm 0.30 \text{ \AA}$ for P. Although the N-distributions in the two halves of the bilayer are slightly asymmetric, those for O and P are not significant.

The above distributions can be compared with those obtained from the GS/DMPC simulation. In the O distribution in the GS layer two peaks, situated at 8 Å and 13 Å, are present. Both were fitted with a Gaussian and their population ratio found to be $\sim 1:7$. The distance between center of the larger, outer Gaussian and that on the opposite monolayer is $26.49 \pm 0.22 \text{ \AA}$, compared with $28.88 \pm 0.32 \text{ \AA}$ for the control system. The same distances for the P-peaks are $33.67 \pm 0.31 \text{ \AA}$ and $37.24 \pm 0.29 \text{ \AA}$, and for N are $35.87 \pm 0.30 \text{ \AA}$ and $36.45 \pm 0.48 \text{ \AA}$. Taken together, these figures suggest that the width of the bilayer is slightly but significantly reduced in the GS/DMPC system.

Interaction energies

Thermograms of GS/DMPC mixtures have been graphically resolved into components attributed to “free” lipids and those “perturbed” by the interaction with GS (Wu et al., 1978). To find an approximate simulation equivalent the non-bonded interaction energies between GS and the individual lipid molecules were examined (Fig. 8). A continuous range of interaction energies is seen. Nine lipids from the GS-layer have average interaction energies greater than $k_B T$, and in what follows these are considered as “bound” to the GS. The remaining eight GS-layer lipids are “free,” as are the 21 from the non-GS layer.

Interestingly, the polar residue/lipid interactions are not mainly electrostatic. For example, $>70\%$ of the van der Waals interaction energy between GS and DMPC 1

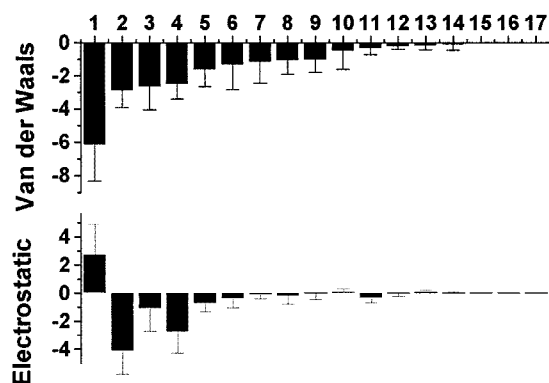


FIGURE 8 Average and standard deviations of the non-bonded interaction energies (in kcal/mol) between GS and each of the DMPC molecules from the layer containing GS.

(-6.2 ± 2.2 kcal/mol) comes from the interaction with Orn-10 (-4.4 ± 1.2 kcal/mol) and this contribution is larger than the electrostatic component, which is -3.3 ± 1.8 kcal/mol. The average electrostatic interaction energy between GS and DMPC 1 is positive, 2.9 ± 1.0 kcal/mol.

Solvation of GS

In Fig. 9 are plotted the numbers of lipid groups (head or tail) and water molecules that are in the proximity of each amino acid residue of GS. Leu and Val are the only residues with no headgroup interactions, consistent with their non-polar nature. The number of nonpolar tail groups close to the polar Orn-10 is maybe surprisingly large. However, this complex environment found for Orn-10 is similar to that observed for a Lys residue during the MD simulation of melittin in a DMPC bilayer (Berneche et al., 1998). The nitrogen atoms of Orn are involved in flickering intramolecular H-bonds with Phe (Fig. 5).

Fig. 9 also shows that the environment of the two halves of the GS molecule is not symmetric. For example, Phe-7

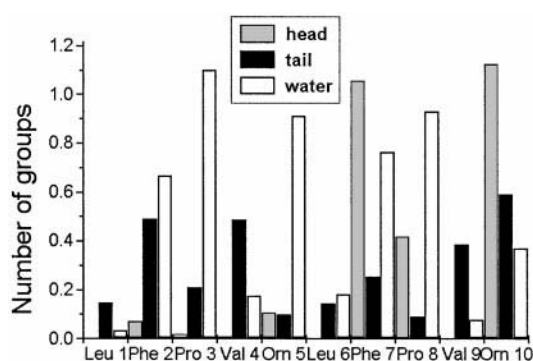


FIGURE 9 Solvation numbers of each amino acid of GS calculated by integrating the pair-to-pair distribution function of the amino acid to the corresponding group between 0 and 4.5 Å.

and Orn-10 are situated closer to the hydrophilic lipid headgroups than Phe-2 and Orn-5. The two aromatic residues were both initially positioned at the membrane/water interface. During the simulation Phe-7 remained in the proximity of the headgroups while Phe-2 moved deeper into the membrane. The environmental asymmetry of the two halves of GS is consistent with the small residual non-convergence of the main-chain and side-chain sequence-symmetric dihedral angle pairs (Fig. 3 B).

Two-dimensional NOESY experiments on model membranes have provided evidence for intense cross-peaks between distant protons such as those of the headgroup choline and the terminal methyl group of lipid hydrocarbon chains (Forbes et al., 1988; Halladay et al., 1990; Huster et al., 1999). This may in principle reflect either close approach of protons in space (i.e., molecular disorder) or spin diffusion (Halladay et al., 1990; Volke and Pampel, 1995), although it appears to be unlikely that the latter effect contributes (Huster et al., 1999; Huster and Gawrisch, 1999). In the present simulations only one lipid terminal methyl group, in the non-GS-layer of the DMPC/GS simulation, came transiently within 6 Å of a headgroup, the latter belonging to another group in the same layer, suggesting that this type of event is very rare in the present simulation model.

Correlation times and order parameter profiles

^2H -NMR provides two distinct kinds of information on membranes: orientational order and fluidity (Bloom et al., 1991). No simple relationship between the two quantities is known for a lipid bilayer (Seelig, 1977). Fluidity here refers to the rate of motion and not to the ordering of the molecular system, as exemplified by the so-called glass-type materials that are disordered but rigid. From a simulation trajectory both properties can be evaluated.

The order parameter of the carbon-deuterium bond, S_{CD} , is defined by $S_{\text{CD}} = \langle 1/2 (3 \cos^2 \theta(t) - 1) \rangle$, where $\theta(t)$ is the angle between the carbon-deuterium bond vector and the bilayer normal; " $\langle \rangle$ " means "time average." Fig. 10 A presents experimental and simulation-derived order parameters for the sn-2 chains of the control system. With one exception (the C2 atom) the order parameters in the control simulation are close to experiment. For C2 experiment suggests the presence of two long-living conformations: the relatively long convergence times for this carbon may contribute to the difference with experiment for C2 seen here and in previous simulations (Tieleman and Berendsen, 1996).

In the GS/DMPC simulation the order parameters of the free lipids from the non-GS and GS layers are rather similar, and the two were subsequently averaged. The free lipids are significantly more ordered than the lipids from the control simulation whereas, clearly, the bound lipids are much more disordered. For both kinds of lipids, an ensemble average

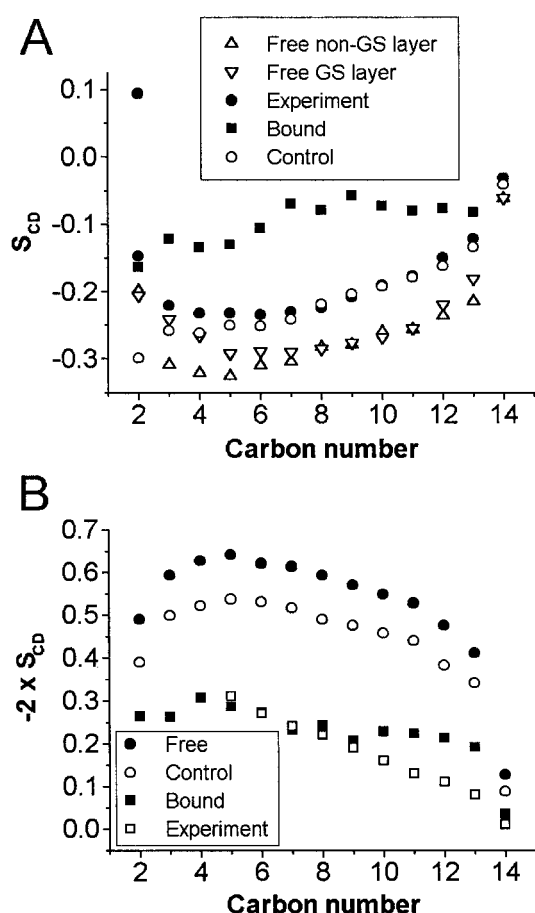


FIGURE 10 (A) Order parameters of the sn-2 chains of DMPC: “free” lipids in layer with GS (∇); “free” lipids from the layer without GS (Δ); control simulation (\circ); “bound” lipids (\blacksquare); and NMR experimental results for the sn-2 of hydrated DMPC bilayers (\bullet) (Douliez et al., 1995). (B) Molecular order parameter ($= -2S_{CD}$) averaged between the chains sn-1 and sn-2 of DMPC: “free” lipids (\bullet); control simulation (\circ); “bound” lipids (\blacksquare); and derived from NMR quadrupole splitting experiments on fully deuterated multilamellar dispersions of DMPC doped with GS (\square) (Zidovetzki et al., 1988).

and a time average for the two lipid tails was calculated to obtain the molecular order parameter plots ($-2S_{CD}$) in Fig. 10 B. The figure also shows experimental data obtained using NMR quadrupole splitting experiments on fully deuterated multilamellar dispersions of DMPC doped with GS at a molar ratio of 1:5.5 at 305 K (Zidovetzki et al., 1988). The results show again that the free lipids are more ordered than in the control simulation. The bound lipid order parameters are close to the experimental values of Zidovetzki et al. (1988). Clearly, the lipids interacting with GS are more disordered.

The narrowing of the width distribution for the headgroup O, N, and P atom distributions in the GS simulation (Fig. 7) suggests that peptide might be ordering the phospholipid headgroups. To verify this the order parameters of the CH bonds of the two methylene groups between the phosphate

and ammonium groups in the lipid heads were computed. The results (not shown) indicate that bound lipid headgroups have a similar order to the control, whereas the free lipids are significantly more ordered.

NMR relaxation parameters probe angular correlation functions of the relaxing nucleus. These correlation functions and their Fourier transforms, the spectral densities, can be obtained directly from MD trajectories. For an ^{13}C nucleus in a DMPC tail the geometrical quantities of interest are spherical polar coordinates (with respect to a laboratory frame) of the C-H internuclear vectors. The T_1 values were computed from this using the equations given in Levy et al. (1981) and Brüschweiler et al. (1992). The required correlation functions reached plateau values in a few hundreds of picoseconds (data not shown).

If the anisotropy of the motion is neglected and the motion assumed to fall into the extreme narrowing limit of the NMR resonance ($\omega_0^2 \tau_c^2 \ll 1$; ω_0 is the resonance frequency) then T_1 and τ_c are the quadrupole spin-lattice relaxation time and the rotational correlation time of the lipids, respectively, assuming that T_1 is independent of the vesicle tumbling rate, the following equation may be written (Brown et al., 1979):

$$1/T_1 = 3/8(e^2qQ/\hbar)^2(1 - S_{CD}^2)\tau_c$$

In the above equation (e^2qQ/\hbar) denotes the static quadrupole constant (170 kHz for carbon-deuterium bonds). Using this equation the T_1 values were used to compute τ_c assuming $(1 - S_{CD}^2) \sim 1$.

The calculated τ_c are plotted in Fig. 11 A together with experimental values obtained from quadrupole spin-lattice relaxation times, T_1 , of deuterium-labeled DPPC bilayer, at 51°C (Brown et al., 1979). The experiment and simulation are in approximate agreement. Fig. 11 A also shows that the fluidity of the bound lipids is increased. The origin of the increased fluidity is a priori unknown. However, one possibility lies in the dihedral transitions. These are plotted in Fig. 11 B for the bound, free, and control lipid tails. The differences between the total numbers of transitions are small, although a slightly higher number of transitions is observed for the bound lipids, consistent with the increased fluidity.

Electrostatic potential

The electrostatic potential difference from the center of the membrane may play a role in ion permeability (Brockman, 1994). Phloretin and gramicidin A are known to affect this potential difference (Cseh and Benz, 1999; Shapovalov et al., 1999). The potential profile was calculated by integrating the charge density as follows:

$$\Psi(z) - \Psi(0) = - \int_0^z dz' \int_0^{z'} \rho(z'') dz'' / \epsilon$$

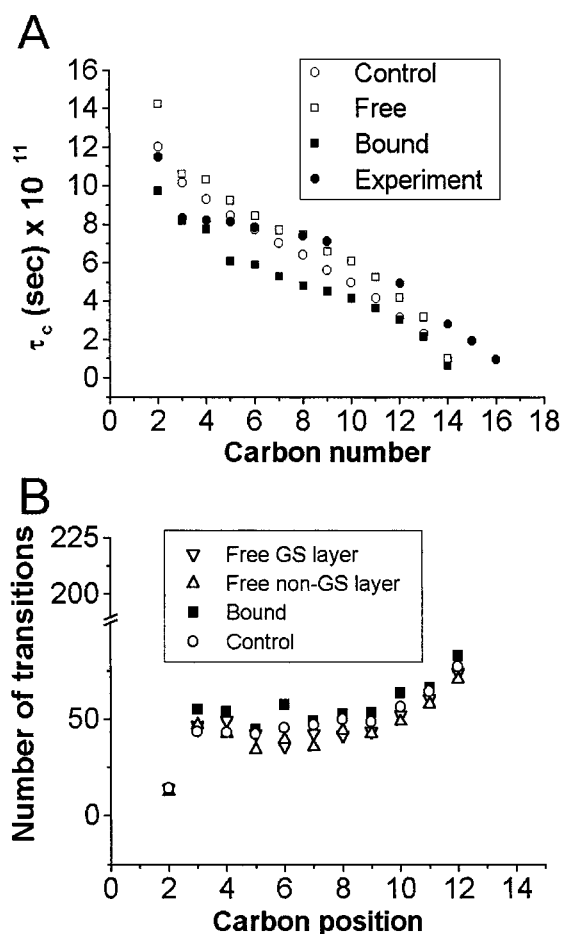


FIGURE 11 (A) Average correlation time for the GS simulation of the lipid chain “free” (□), control simulation (○), “bounded” lipids (■), and experimental replotted from Brown et al. (1979). (B) Transition number of the tails of DMPC: “free” lipids in layer with GS (▽), “free” lipids from the layer without GS (△), control simulation (○), and “bounded” lipids. A transition is defined here as crossing at least 30° beyond the potential maximum between wells. The angles considered are defined by the dihedrals $C_{i-1}-C_i-C_{i+1}-H'$ or $C_{i-1}-C_i-C_{i+1}-H''$, where H' and H'' are the two methylene hydrogens. The rotational energies of these dihedrals have three minima at 60° , -60° , and 180° . The total number of lipid tail dihedral transitions was counted and the number in the control simulation multiplied by 3/2 to account for the difference in simulation lengths.

where $\Psi(z)$ denotes the electrostatic potential and $\rho(z)$ the charge density. The total and component electrostatic membrane dipole potentials for GS-DMPC and control systems are shown in Fig. 12. In the present study, values closer to experiment were obtained if the dielectric constant, ϵ was considered equal to $2\epsilon_0$, where ϵ_0 is the vacuum permittivity. The same approach was used in Tieleman and Berendsen (1996) while other studies have considered $\epsilon = \epsilon_0$ (for example, Essemann and Berkowitz, 1999).

The total dipole potentials for the GS/DMPC and control systems in Fig. 12 are very similar. For both simulations, values ~ -0.6 V are obtained, with the membrane interior positive compared to the exterior. Experimentally, this

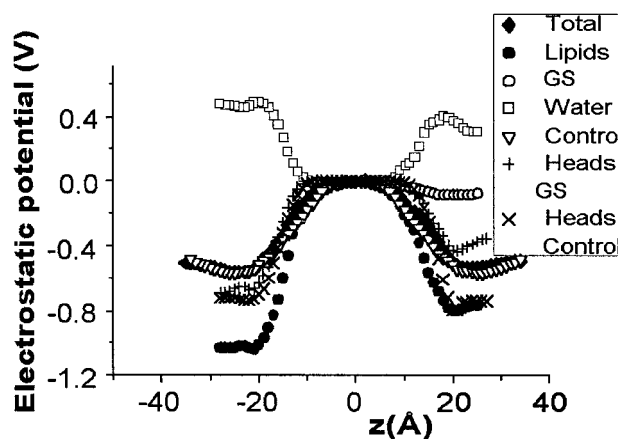


FIGURE 12 The total membrane potentials for the GS containing system, control simulation, and the contributions due to lipids, water, and GS for the GS-DMPC-water system. The sizes of the symbols are proportional to the standard deviations of the quantities. $\psi(0)$ is taken as zero at $z = 0$.

quantity is rather difficult to obtain (Brockman, 1994). Measurements on PC/water interfaces have obtained somewhat lower values, between -0.2 V (Gawrisch et al., 1992) and -0.4 V (Pickar and Benz, 1978).

As discussed above, there is a change in the headgroup orientation in the GS layer. Fig. 12 shows that this change is reflected in the headgroup contribution to the dipole potential, which differs significantly from the control. The contribution of GS itself to the total membrane dipole potential is small. The total dipole potential computed from the DMPC-GS simulation remains symmetric and close to that of the control, due in part to compensation of the effects of asymmetry in the contributions of lipids and water. Indeed, it has been suggested that reorientation of the water can play a significant role in balancing the dipole potential (Essemann and Berkowitz, 1999).

Water

Finally, we examine the water molecule distributions in the two simulations. These are given in Fig. 13, A and B. The number of water molecules outside the membrane is different because the two systems contain different total numbers of water molecules, having been initially constructed with the same size. The distributions in the control and GS/DMPC simulations are similar. However, a small but significant asymmetric feature is observed within the GS/DMPC system, illustrated in Fig. 13C in which the difference between the time-averaged number of water molecules in opposite monolayers is plotted (positive z is the GS layer). The positive difference indicates that more water molecules penetrate into the non-GS layer. From a total of 1666 water molecules in the system, only four penetrated to within 3 Å of the center at any moment during the trajec-

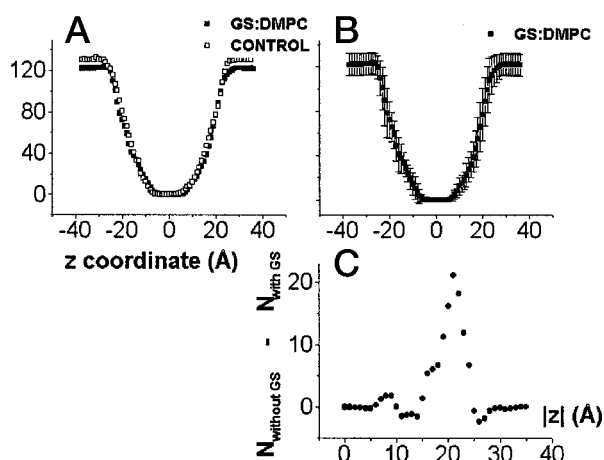


FIGURE 13 Water molecule distributions. The bilayer center is at $z = 0$. A. Average number of water molecules as a function of z in the GS/DMPC and control simulations. The number of water molecules outside the membrane is different because the two systems contain different total numbers of water molecules, having been initially constructed with the same size. B. Average and standard deviation for the GS/DMPC system. C. Difference in the average number of water molecules laying in sections equidistant from $z = 0$ in the non-GS and GS-layers of the GS/DMPC simulation.

tory, these making only transient visits. None of these actually cross the membrane.

CONCLUSIONS

The approach taken in the present work on peptide/membrane interaction was to perform a control simulation of a hydrated model phospholipid bilayer and to investigate perturbative effects of a peptide on it in a second simulation. It is encouraging that the variety of properties of the control (hydrated DMPC) simulation examined are in overall agreement with experiment (area per lipid, lipid tail order parameters, quadrupole spin-lattice relaxation times), giving confidence in the simulation methodology and in the description it affords of the qualitative changes induced by GS.

The simple C2-symmetric cyclic GS decapeptide has significantly limited conformational flexibility, and its experimentally observed antiparallel β -sheet conformation with two Type II' β -turns is rigidly retained over the 3-ns length of the present simulation. This conformation leads to an amphipathic "sidedness" in the side-chain orientations and, after an excursion during the initial equilibration, GS returns to its initial orientation and position at the polar interface and remains there. The main-chain dihedrals are close to those of NMR experiment on GS in DMSO. Of particular interest is the observation that sequence-symmetric main-chain and side-chain dihedral angle pairs gradually converge to within $\sim 5^\circ$ and $\sim 10^\circ$, respectively, on the time scale examined.

The effects of gramicidin S on the membrane structure and dynamics are smaller than have been seen in some peptide/membrane simulations. For example, in the work on the melittin-DMPC system significant local thinning of the bilayer was seen (Berneche et al., 1998); this may be related to the significantly larger size of melittin (26 residues). GS has little effect on the electrostatic potential difference between the center and outside of the membrane and there is no noticeable effect on the water permeability over the accessible time scale. There is, therefore, no clear indication from the present simulation as to how GS affects membrane permeability. This is not surprising, as the GS/lipid ratio here is significantly lower than would be required for permeability effects to be clearly detectable experimentally. Moreover, as only a single GS molecule is included in the system, the present simulations do not allow mechanisms involving peptide-peptide associations to be probed.

However, lipid perturbation by a single GS molecule is clearly an essential first step toward understanding permeability effects. For example, pore formation has been suggested to occur due to the bilayer-disturbing mechanisms of amphipathic peptides (Bechinger, 1999). Here, a significant reduction in the solvent-accessible area per lipid is seen in both the non-GS-containing and GS-containing layers of the GS/DMPC system. This may be relevant for explaining electron paramagnetic resonance data that indicate that GS decreases the amount of an amphiphilic spin label (Tempo) incorporated into the hydrophobic regions of phospholipid vesicles (Hubbel and McConnell, 1968). It was speculated that GS might tend to freeze the otherwise fluid hydrophobic regions and therefore to decrease the volume available to the amphipathic label, consistent with the present findings. However, as discussed in the Results section, the result for the area per lipid in the peptide-containing layer depends on whether the peptide cross-sectional area is included.

In the present work GS has a small but significant effect on membrane thickness here, but no clear effect on membrane curvature, which is also of interest in light of the suggestion that localized increases in membrane monolayer curvature stress may be part of the mechanism through which GS exhibits its antimicrobial and hemolytic activities (Prenner et al., 1997).

The "bound" lipids are more disordered (in agreement with NMR experiment) and more fluid, an effect that has been observed for almost all the lipid-protein interactions studied so far by NMR and computer simulation techniques, an exception being the MD studies on gramicidin A in DMPC (Woolf and Roux, 1996; Chiu et al., 1999). The lipids in the GS/DMPC system not interacting with GS are ordered relative to the control lipids. The possibility that this is a simulation artefact cannot be ruled out, as long-range collective effects may be sensitive to system size, simulation length, force field, and pressure effects. However, this intriguing indirect effect certainly merits further investigation.

REFERENCES

- Balasubramanian, D. 1967. The conformation of gramicidin S in solution. *J. Am. Chem. Soc.* 89:5445–5449.
- Bechinger, B. 1999. The structure, dynamics and orientation of antimicrobial peptides in membranes by multidimensional solid-state NMR spectroscopy. *Biochim. Biophys. Acta.* 1462:157–183.
- Berneche, S., M. Nina, and B. Roux. 1998. Molecular dynamics simulation of melittin in a dimyristoylphosphatidylcholine bilayer membrane. *Biophys. J.* 75:1603–1618.
- Bloom, M., E. Evans, and O. G. Mouritsen. 1991. Physical properties of the fluid lipid-bilayer component of cell membranes: a perspective. *Q. Rev. Biophys.* 24:293–397.
- Brockman, H. 1994. Dipole potential of lipid membranes. *Chem. Phys. Lipids.* 73:57–79.
- Brooks, B. R., R. E. Bruccoleri, B. D. Olafson, D. J. States, S. Swaminathan, and M. Karplus. 1983. CHARMM: a program for macromolecular energy, minimization and dynamics calculations. *J. Comp. Chem.* 4:187–217.
- Brown, M. F., J. Seelig, and U. Haberland. 1979. Structural dynamics in phospholipid bilayers from deuterium spin-lattice time measurements. *J. Chem. Phys.* 70:5045–5053.
- Brüschweiler, B., B. Roux, M. Blackledge, C. Griesinger, M. Karplus, and R. R. Ernst. 1992. Influence of rapid intramolecular motion on NMR cross-relaxation rates. A molecular dynamics study of antamanide in solution. *J. Am. Chem. Soc.* 114:2289–2302.
- Chiu, S.-W., S. Subramaniam, and E. Jakobsson. 1999. Simulation study of a gramicidin/lipid bilayer system in excess water and lipid. I. Structure of the molecular complex. *Biophys. J.* 76:1929–1938.
- Cseh, R., and R. Benz. 1999. Interaction of phloretin with lipid monolayer; relationship between structural changes and dipole potential change. *Biophys. J.* 77:1477–1488.
- Datema, K. P., K. P. Pauls, and M. Bloom. 1986. Deuterium nuclear magnetic resonance investigation of the exchangeable sites on gramicidin A and gramicidin S in multilamellar vesicles of dipalmitoylphosphatidylcholine. *Biochemistry.* 25:3796–3803.
- Davis, J. H., D. M. Clare, R. S. Hodges, and M. Bloom. 1983. Interaction of a synthetic amphiphilic polypeptide and lipids in a bilayer structure. *Biochemistry.* 22:5298–5305.
- Douliez, J.-P., A. Leonard, and E. J. Dufourc. 1995. Restatement of order parameters in biomembranes: calculation of C-C bond order parameters from C-D quadrupolar splittings. *Biophys. J.* 68:1727–1739.
- Esseemann, U., and M. L. Berkowitz. 1999. Dynamical properties of phospholipid bilayers from computer simulation. *Biophys. J.* 76:2081–2089.
- Feller, S. E., and R. W. Pastor. 1996. On simulating lipid bilayers with an applied surface tension: periodic boundary conditions and undulations. *Biophys. J.* 71:1350–1355.
- Feller, S. E., Y. Zhang, R. W. Pastor, and B. R. Brooks. 1995. Constant pressure molecular dynamic simulation: the Langevin piston method. *J. Chem. Phys.* 103:4613–4621.
- Forbes, J. C., C. Husted, and E. Oldfield. 1988. High-field, high-resolution proton “magic-angle” sample-spinning nuclear magnetic resonance spectroscopic studies of gel and liquid crystalline lipid bilayer and the effects of cholesterol. *J. Am. Chem. Soc.* 110:1059–1065.
- Gawrisch, K., D. Ruston, J. Zimmerberg, V. A. Parsegian, R. P. Rand, and N. Fuller. 1992. Membrane dipole potentials, hydrogen forces, and the ordering of water at membrane surface. *Biophys. J.* 61:1213–1223.
- Halladay, H. N., R. E. Stark, S. Ali, and R. Bittman. 1990. Magic-angle spinning NMR studies of molecular organization in multibilayers formed by 1-octadecanoyl-2-decanoyl-sn-glycero-3-phosphocholine. *Biophys. J.* 58:1449–1461.
- Higashijima, T., T. Miyazawa, M. Kawai, and U. Nagai. 1986. Gramicidin S analogues with D-Ala, Gly, or L-Ala residues in place of the D-Phe residue: molecular conformations and interactions with phospholipid membrane. *Biopolymers.* 25:2295–2307.
- Hubbel, W. L., and H. M. McConnell. 1968. Spin-label studies of the excitable membranes of nerve muscle. *Proc. Natl. Acad. Sci. U.S.A.* 61:12–16.
- Hull, E., R. Karlsson, P. Main, M. M. Woolfson, and E. J. Dodson. 1978. The crystal structure of a hydrated gramicidin S-urea complex. *Nature.* 275:206–207.
- Huster, D., K. Arnold, and K. Gawrisch. 1999. Investigation of lipid organization in biological membranes by two-dimensional nuclear Overhauser enhancement spectroscopy. *J. Phys. Chem. B.* 103:243–251.
- Huster, D., and K. Gawrisch. 1999. NOESY NMR crosspeaks between lipid headgroups and hydrocarbon chains: spin diffusion or molecular disorder? *J. Am. Chem. Soc.* 121:1992–1993.
- Jähnig, F. 1996. What is the surface tension of a lipid bilayer membrane? *Biophys. J.* 71:1348–1349.
- Jones, C. R., C. T. Sikakana, S. Hehir, M.-C. Kuo, and W. A. Gibbons. 1978. The quantitation of nuclear Overhauser effect methods for total conformational analysis of peptides in solution. Application to gramicidin S. *Biophys. J.* 24:815–832.
- Jorgensen, W. L., J. Chandrasekhar, J. D. Madura, R. N. Impey, and M. L. Klein. 1983. Comparison of simple potential functions for simulating liquid water. *J. Chem. Phys.* 79:926–935.
- Katsu, T., H. Kobayashi, T. Hirota, Y. Fujita, K. Sato, and U. Nagai. 1987. Structure-activity relationship of gramicidin S analogues on membrane permeability. *Biochim. Biophys. Acta.* 899:159–170.
- Katsu, T., M. Kuroko, T. Morikawa, K. Sanchika, Y. Fujita, H. Yamamura, and M. Uda. 1989. Mechanism of membrane damage induced by amphipathic peptides gramicidin S and melittin. *Biochim. Biophys. Acta.* 983:135–141.
- König, W., H. H. Strey, and K. Gawrisch. 1997. Membrane lateral compressibility determined by NMR and x-ray diffraction: effect of acyl chain polysaturation. *Biophys. J.* 73:1954–1966.
- Krauss, E. M., and S. I. Chan. 1982. Intramolecular hydrogen bonding in gramicidin S. 2. Ornithine. *J. Am. Chem. Soc.* 104:6953–6961.
- Lee, B., and F. M. Richards. 1971. The interpretation of protein structures: estimation of static accessibility. *J. Mol. Biol.* 55:379–400.
- Levy, R. M., M. Karplus, and P. G. Wolynes. 1981. NMR relaxation parameters in molecules with internal motion: exact Langevin trajectory results compared with simplified relaxation models. *J. Am. Chem. Soc.* 103:5998–6011.
- MacKerell, Jr., A. D., D. Bashford, M. Bellott, R. L. Dunbrack, Jr., J. D. Evensen, M. J. Field, S. Fischer, J. Gao, H. Guo, S. Ha, D. Joseph-McCarthy, L. Kuchnir, K. Kucera, F. T. K. Lau, C. Mattos, S. Michnick, T. Ngo, D. T. Nguyen, B. Prodhom, I. W. E. Reiher, B. Roux, M. Schlenkerich, J. C. Smith, R. Stote, J. Straub, M. Watanabe, J. Wierkiewicz-Kucera, D. Yin, and M. Karplus. 1998. All-atom empirical potential for molecular modeling and dynamics studies of proteins. *J. Phys. Chem. B.* 102:3586–3616.
- Marrink, S. J., M. Berkowitz, and H. J. C. Berendsen. 1993. Molecular dynamics simulation of a membrane water interface—the ordering of water and its relation to the hydration force. *Langmuir.* 9:3122–3131.
- Mihailescu, D., and J. C. Smith. 1999. Molecular dynamics simulation of the cyclic decapeptide antibiotic, gramicidin S, in dimethyl sulfoxide solution. *J. Phys. Chem. B.* 9:1586–1594.
- Nagle, J. F., R. Zhang, S. Tristram-Nagle, W. Sun, H. I. Petrache, and R. M. Suter. 1996. X-ray structure determination of fully hydrated L_{α} phase dipalmitoylphosphatidylcholine bilayers. *Biophys. J.* 70:1419–1431.
- Ovchinnikov, Y. A., and V. T. Ivanov. 1975. Conformational states and biological activity of cyclic peptides. *Tetrahedron.* 31:2177–2185.
- Pache, U., D. Chapman, and R. Hillaby. 1972. Interaction of antibiotics with membranes: polymyxin B and gramicidin S. *Biochim. Biophys. Acta.* 255:358–364.
- Petrache, H. I., S. Tristram-Nagle, and J. F. Nagle. 1998. Fluid phase structure of EPC and DMPC bilayers. *Chem. Phys. Lipids.* 95:83–94.
- Pickar, A. D., and R. Benz. 1978. Transport of oppositely charged lipophilic probe ions in lipid bilayer membranes having various structure. *J. Membr. Biol.* 44:353–376.
- Portlock, S. H., M. J. Clague, and R. J. Cherry. 1990. Leakage of internal markers from erythrocytes and lipid vesicles induced by melittin, gramicidin S and alamethicin: a comparative study. *Biochim. Biophys. Acta.* 1030:1–10.

- Prenner, E. J., R. N. A. H. Lewis, K. C. Neuman, S. M. Gruner, L. H. Kondejewski, R. S. Hodges, and R. N. McElhaney. 1997. Nonlamellar phase induced by the interaction of gramicidin S with lipid bilayers. A possible relationship to membrane-disrupting activity. *Biochemistry*. 37: 7906–7916.
- Roux, B., and T. B. Woolf. 1996. Molecular dynamics of Pfl coat protein in phospholipid bilayer. In *Biological Membranes. A Molecular Perspective from Computation and Experiment*. K. M. Merz and B. Roux, editors. Birkhauser, Boston. 555–587.
- Schlenkerich, M. J., J. Brickmann, A. D., MacKerell, Jr., and M. Karplus. 1996. An empirical potential energy function for phospholipids: criteria for parameters optimization and applications. In *Biological Membranes. A Molecular Perspective from Computation and Experiment*. K. M. Merz and B. Roux, editors. Birkhauser, Boston. 31–81.
- Seelig, J. 1977. Deuterium magnetic resonance: theory and application to lipid membranes. *Q. Rev. Biophys.* 10:353–418.
- Shapovalov, L., E. A. Kotova, T. I. Rokitskaya, and Y. N. Antonenko. 1999. Effect of gramicidin A on the dipole potential of phospholipid membranes. *Biophys. J.* 77:299–305.
- Stern, A., W. A. Gibbons, and L. C. Craig. 1968. A conformational analysis of gramicidin S-A by nuclear magnetic resonance. *Proc. Natl. Acad. Sci.* 61:734–741.
- Stouch, T. R. 1993. Lipid membrane structure and dynamics studied by all-atom molecular dynamics simulations of hydrated phospholipid bilayer. *Mol. Sim.* 10:335–362.
- Tieleman, D. P., and H. J. C. Berendsen. 1996. Molecular dynamics simulation of a fully hydrated dipalmitoylphosphatidylcholine bilayer with different macroscopic boundary conditions and parameters. *J. Phys. Chem.* 105:4871–4880.
- Tieleman, D. P., S. J. Marrink, and H. J. C. Berendsen. 1997. A computer perspective of membranes: molecular dynamics studies of lipid bilayer systems. *Biochim. Biophys. Acta.* 1331:235–270.
- Venable, R. M., Y. Zhang, B. J. Hardy, and R. W. Pastor. 1993. Molecular dynamics simulations of a lipid bilayer and of hexadecane: an investigation of membrane fluidity. *Science*. 262:223–226.
- Volke, F., and A. Pampel. 1995. Membrane hydration and structure on a subnanometer scale as seen by high resolution solid state nuclear magnetic resonance: POPC and POPC/C12 EO4 model membranes. *Biophys. J.* 68:1960–1965.
- Woolf, T. B. 1998. Molecular dynamics simulation of individual α -helices of bacteriorhodopsin in dimyristoylphosphatidylcholine. II. Interaction energy analysis. *Biophys. J.* 74:115–131.
- Woolf, T. B., and B. Roux. 1994. Molecular dynamics simulation of the gramicidin channel in a phospholipid bilayer. *Proc. Natl. Acad. Sci. U.S.A.* 91:11631–11635.
- Woolf, T. B., and B. Roux. 1996. Structure, energetics and dynamics of lipid-protein interactions: a molecular dynamics study of the gramicidin A channel in a DMPC bilayer. *Proteins*. 24:92–114.
- Wu, E.-S., K. Jacobson, F. Szoka, and A. Portis, Jr. 1978. Lateral diffusion of a hydrophobic peptide, N-4-nitrobenz-oxa-1,3-diazole gramicidin S, in phospholipid multibilayers. *Biochemistry*. 17:5543–5550.
- Xu, Y., I. P. Sugar, and N. R. Krishna. 1995. A variable target intensity-restrained global optimization (VARTIGO) procedure for determining three-dimensional structure of polypeptides from NOESY data: application to gramicidin-S. *J. Biomol. NMR*. 5:37–48.
- Zidovetzki, R., U. Banerjee, D. W. Harrington, and S. I. Chan. 1988. NMR study of the interaction of polymyxin B, gramicidin S, valinomycin with dimyristoyllecithin bilayers. *Biochemistry*. 27:5686–5692.